Optimal Lyapunov-based quantum control for quantum systems

S. C. Hou, M. A. Khan, X. X. Yi, Daoyi Dong, and Ian R. Petersen

Phys. Rev. A **86**, 022321 — Published 21 August 2012

DOI: 10.1103/PhysRevA.86.022321

Optimal Lyapunov-based quantum control for quantum systems

S. C. Hou, M. A. Khan, X. X. Yi,
School of Physics and Optoelectronic Technology,
Dalian University of Technology, Dalian 116024, China

Daoyi Dong, Ian R. Petersen
School of Engineering and Information Technology,
University of New South Wales at the Australian Defence Force Academy, Canberra, ACT 2600, Australia
(Dated: July 5, 2012)

Quantum Lyapunov control was developed in order to transform a quantum system from arbitrary initial states to a target state. The idea is to find control fields that steer the Lyapunov function to zero as $t \to \infty$, meanwhile the quantum system is driven to the target state. In order to shorten the time required to reach the target state, we propose two designs to optimize Lyapunov control in this paper. The first design makes the Lyapunov function decrease as fast as possible with a constraint on the total power of control fields, and the second design has the same purpose but with a constraint on each control field. Examples of a three-level system demonstrate that the evolution time for Lyapunov control can be significantly shortened, especially when high control fidelity is required. Besides, this optimal Lyapunov-based quantum control is robust against uncertainties in the free Hamiltonian and decoherence in the system compared to conventional Lyapunov control. **We apply our optimal design to cool a nanomechanical resonator, a shorter cooling time is found with respect to the cooling time by the conventional Lyapunov design.**

PACS numbers: 03.65.Yz, 02.30.Yy, 03.67.-a

I. INTRODUCTION

Quantum control [1, 2] has attracted much attention in recent years and it has found potential applications in many fields such as quantum information processing, quantum chemistry and quantum simulation. Among these quantum control problems, state transfer is a central task. Various methods such as quantum optimal control and Lie group decompositions have been used to design control laws to drive quantum systems to target states or to realize some specific operations [3–13].

Quantum Lyapunov control was proposed in the early 2000s as a good candidate for state transfer[14, 15]. This strategy has been widely studied recently both in theory and applications [16–26], because it offers a simple and effective way to design control fields. However, the problem of speeding up Lyapunov control has not been widely considered to date. Quantum Lyapunov control is practically employed in an open-loop way without measurement and feedback. Hence, it is quite natural to shorten the evolution time so as to overcome the decoherence effect induced by inevitable interactions with the surrounding environment.

In quantum Lyapunov control, a function V, called a Lyapunov function of quantum states, is specified to design time-varying control fields. The system converges to the target state given by $\dot{V} = 0$ while V decreases to its minimum. Based on this concept, we present a scheme to optimize Lyapunov control by using the following idea: Speed up evolution to the target state by making V decrease faster.

Generally, the total Hamiltonian in a quantum control system can be written in two parts $H_0 + \sum_{n=1}^{k} f_n(t)H_n$, where H_0 is the free (internal) Hamiltonian and H_n are external control Hamiltonians with $f_n(t)$ representing the corresponding control fields. These control fields should be designed to ensure $\dot{V} \leq 0$. In fact, there are many ways to choose $f_n(t)$ to achieve this goal. In this paper, we consider the question: With given control Hamiltonians H_n, how should we design the shape of the control fields $f_n(t)$ in order to make V decrease fastest.

It is shown that one can enable V to decrease faster simply by enhancing the strength of the control fields. However, strong control fields may not be feasible and always bring unwanted results, for example a large energy (power) cost, invalidation of mathematical approximation and treatment for the system. In view of these factors, we propose two designs for the control fields. One is under the constraint that the power-type quantity $W = \sum_{n=1}^{k} f_n(t)^2$ is bounded. The other is under the constraint that the strength of each field is bounded. These designs for control fields make V decrease as fast as possible within given limitations. The second design has the simple form of "bang-bang" control which is easy to be implemented in an experiment. We also illustrate our control method with a three-level system. The results suggest that the evolution time is significantly reduced compared with the conventional method.

The paper is organized as follows: In Sec.II, we derive control fields for a general Lyapunov function $V = \mathrm{Tr}(P\rho)$ under the two aforementioned constraints. In Sec.III, we simulate our field designs and compare them with the conventional method. The robustness of the optimal Lyapunov designs is analyzed in Sec.IV. Finally, we summarize our work in Sec. V.

II. DESIGN OF CONTROL FIELDS

In quantum Lyapunov control, the system is steered from an initial state to a target state by control fields designed using Lyapunov function V. The goal of this paper is to obtain optimized control fields that make the time derivative of the Lyapunov function $|\dot{V}|$ largest so as to speed up the evolution to the target state. We start from a closed quantum system described by the Liouville equation

$$\frac{d\rho}{dt} = -i[H_0 + H_c(t), \rho], \tag{1}$$

where H_0 is the free Hamiltonian for the controlled system and $H_c(t)$ is a time-dependent Hamiltonian representing coupling to external control fields which is called the control Hamiltonian. We have set $\hbar = 1$ and assume that the system is controllable. In Lyapunov control, the solution of Eq.(1) converges to the minimum of $V(\rho)$. Meanwhile, the state converges to a set of states characterized by the La Salle's invariance principle [1]. The control Hamiltonian $H_c(t)$ can be written in the form,

$$H_c(t) = \sum_{n=1}^{k} f_n(t) H_n \tag{2}$$

where H_n $(n = 1, ..., k)$ are time-independent Hermitian operators corresponding to different types of external control and $f_n(t)$ are time-varying real functions, usually representing electro-magnetic fields. k is a positive integer.

In this paper we consider the following form of Lyapunov function

$$V = \mathrm{Tr}(P\rho), \tag{3}$$

where P is a Hermitian operator and assumed to be positive semi-definite in order to satisfy the standard requirement for a Lyapunov function, $V \geq 0$ [1]. Also, some other forms of Lyapunov function can be described by Eq.(3), such as that based on the Hilbert Schmidt distance [1, 19].

The time derivative of V needs to be calculated to design the control fields,

$$\begin{aligned} \dot{V} &= \mathrm{Tr}(-iP[H_0 + \sum_{n=1}^{k} f_n(t) H_n, \rho]) \\ &= \mathrm{Tr}(-i\rho[P, H_0]) + \sum_{n=1}^{k} f_n(t)\mathrm{Tr}(-i\rho[P, H_n]) \\ &= \sum_{n=1}^{k} f_n(t) T_n \end{aligned} \tag{4}$$

where $T_n = \mathrm{Tr}(-i\rho[P, H_n])$ is a real function of ρ, H_n and P. We have used the assumption that $[P, H_0] = 0$, which can be achieved by constructing P using the eigenvectors of H_0.

The Lyapunov control strategy requires $\dot{V} \leq 0$. There are many ways to design $f_n(t)$ to satisfy this requirement. A simple and conventional way is to let $f_n(t) = -KT_n$ with $K > 0$ so that

$$\dot{V}(\rho) = -\sum_{n=1}^{k} KT_n(t)^2 \leq 0. \tag{5}$$

With such control fields, V will decrease to its minimum and state ρ will converge to the target state ρ_f with the same spectrum as the initial state ρ_0 and satisfying $\mathrm{Tr}(e^{-iH_0 t}\rho_f e^{iH_0 t}[P, H_n]) = 0$ [1].

In the conventional field design method, the amplitude of the control fields $f_n(t)$ is proportional to T_n. That means when T_n is small (for example, when ρ is very close to ρ_f), $f_n(t)$ will become small leading to a slow decreasing of V and a long evolution time. Our aim is to determine optimized control fields $f_n(t)$ to enable V to decrease as fast as possible in order to speed up control. From Eq.(4) it is seen that if each $f_n(t)$ has a different sign to the corresponding T_n, then $\dot{V} < 0$ and large $|f_n(t)|$ will lead to fast decreasing of V. Therefore, the problem has to be discussed under a constraint on the control fields $f_n(t)$. Considering the following reasons for constraining the control fields: First, one often wishes control fields to be weak in order to reduce energy (power) costs. Second, strong external control fields may lead to invalidation of the modeling of the system. Third, strong fields may disturb neighboring quantum systems that we do not want to disturb. We propose two designs of control fields under constraints on the power of the control fields (constraint A) and on the strength of each control field (constraint B), respectively.

A. A power-type Constraint

First, we consider the following constraint on the control fields

$$W = \sum_{n=1}^{k} f_n(t)^2 \leq W_{max}. \tag{6}$$

Since the control fields $f_n(t)$ are always associated with the amplitude of the electro-magnetic fields, the quantity W can be interpreted as a power-type quantity. We will call it power for simplicity in the following. The total power of the control fields is bounded in this case.

Consider $\sum_{n=1}^{k} T_n^2 \neq 0$ $(\rho \neq \rho_f)$ in time t and the constraint for $f_n(t)$ is $\sum_{n=1}^{k} f_n(t)^2 = W$. In order to determine the optimized control fields that minimize $\dot{V} = \sum_{n=1}^{k} f_n(t) T_n$ ($\dot{V}$ is negative), we use the Lagrange multiplier method. Let

$$L = \sum_n f_n T_n + \lambda(\sum_n f_n^2 - W) \tag{7}$$

where λ is the Lagrange multiplier, and f_n represents $f_n(t)$ at a certain time t. Then from the following equations

$$\frac{\partial}{\partial f_n}L = T_n + 2\lambda f_n = 0, \tag{8}$$

$$\frac{\partial}{\partial \lambda}L = \sum f_n^2 - W = 0, \tag{9}$$

it is easy to obtain the amplitude of the fields f_n at time t,

$$f_n = -\frac{\sqrt{W}T_n}{\sqrt{\sum_{n=1}^{k} T_n^2}} \tag{10}$$

with $T_n = \mathrm{Tr}(-i\rho[P, H_n])$. The corresponding time derivative of Lyapunov function is

$$\dot{V} = \sum_{n=1}^{k} f_n T_n = -\frac{\sqrt{W}\sum_{n=1}^{k} T_n^2}{\sqrt{\sum_{n=1}^{k} T_n^2}}. \tag{11}$$

It is seen that $\dot{V}$ is proportional to $\sqrt{W}$, so we choose $W = W_{max}$ for a faster decreasing of V and our control design for all evolution time reads

$$f_n(t) = \begin{cases} -\frac{\sqrt{W_{max}}T_n}{\sqrt{\sum_{n=1}^{k} T_n^2}} & (\sum_{n=1}^{k} T_n^2 \neq 0) \\ 0 & (\sum_{n=1}^{k} T_n^2 = 0). \end{cases} \tag{12}$$

Note that when ρ reaches the final state ρ_f, all $T_n = \mathrm{Tr}(-i\rho_f[P, H_n])$ become zero and all control fields are switched off. Considering that ρ converges to ρ_f asymptotically, we will switch off the control fields after $D(\rho, \rho_f) < \varepsilon$ where D denotes some measurement for the distance between ρ and ρ_f and ε is the required precision.

In the case $k = 1$, i.e., there is only one control Hamiltonian, our control design reduces to

$$f_1(t) = \begin{cases} -\sqrt{W_{max}} & (T_1 > 0) \\ \sqrt{W_{max}} & (T_1 < 0) \\ 0 & (T_1 = 0) \end{cases} \tag{13}$$

which has a simple "bang-bang" control form. With its discrete shape of the control fields, this control design should be easy to realize experimentally [8, 23].

B. Constraint on the strength of each control field

Next, we will find the optimized control fields when the strength of each field is bounded. For simplicity, we assume the maximum strength of every control field $f_n(t)$ is S ($S > 0$), i.e.,

$$|f_n(t)| \leq S, \quad (n = 1, 2, \cdots, k). \tag{14}$$

From $\dot{V} = \sum_{n=1}^{k} f_n(t)T_n$, it is easy to obtain the optimized control fields that minimize $\dot{V}$ with condition Eq.(14),

$$f_n(t) = \begin{cases} -S & (T_n > 0) \\ S & (T_n < 0) \\ 0 & (T_n = 0) \end{cases} \quad n = 1, 2, \cdots, k \tag{15}$$

and the time derivative of the Lyapunov function is

$$\dot{V} = \sum_{n=1}^{k} f_n(t)T_n = -S\sum_{n=1}^{k} |T_n|. \tag{16}$$

This design has the "bang-bang" control form with k different control fields. When there is only one control Hamiltonian, the design has the same form as that in Eq.(13) with $\sqrt{W}$ replaced by S.

We have presented two designs of control fields for systems described by Eq.(1) and Lyapunov function Eq.(3) with two constraints. However, these designs can also be applied to other Lyapunov control as long as the derivative of Lyapunov function has the form of Eq.(4) where $f_n(t)$ represents a control field and T_n represents a real function of the quantum state. In fact, for many different kinds of Lyapunov function and different dynamical equations [14, 18, 20, 21], $\dot{V}$ takes this form.

III. ILLUSTRATIONS

In this section, we will present an example to illustrate the proposed schemes. The example consists of a 3-level system driven by a control Hamiltonian. We show that the system can be steered to an eigenstate of the free Hamiltonian from arbitrary initial states (except the states in the La Salle's invariant space) by both the conventional design $f_n(t) = -KT_n$ and the design proposed in this paper. The difference is that the present design can speed up the convergence.

Consider a three-level system described by the quantum Liouville equation

$$\frac{d\rho}{dt} = -i[H_0 + \sum_{n=1}^{4} f_n(t)H_n, \rho] \tag{17}$$

with free Hamiltonian

$$H_0 = \omega \begin{pmatrix} 1.5 & 0 & 0 \\ 0 & 1 & 0 \\ 0 & 0 & 0 \end{pmatrix}. \tag{18}$$

where the energy difference between $|1\rangle$ and $|2\rangle$ ($|2\rangle$ and $|3\rangle$) is ω ($\frac{1}{2}\omega$). $\hbar = 1$ has been set throughout this paper.

The aim is to steer the system from an arbitrary initial pure state $\rho_0 = |\phi_0\rangle\langle\phi_0|$ to an eigenstate, say $|\phi_f\rangle = |3\rangle = [1, 0, 0]^T$ of the free Hamiltonian H_0. We choose the Lyapunov function $V = \mathrm{Tr}(P\rho)$ with

$$P = \begin{pmatrix} 0 & 0 & 0 \\ 0 & 1 & 0 \\ 0 & 0 & 1 \end{pmatrix}. \tag{19}$$

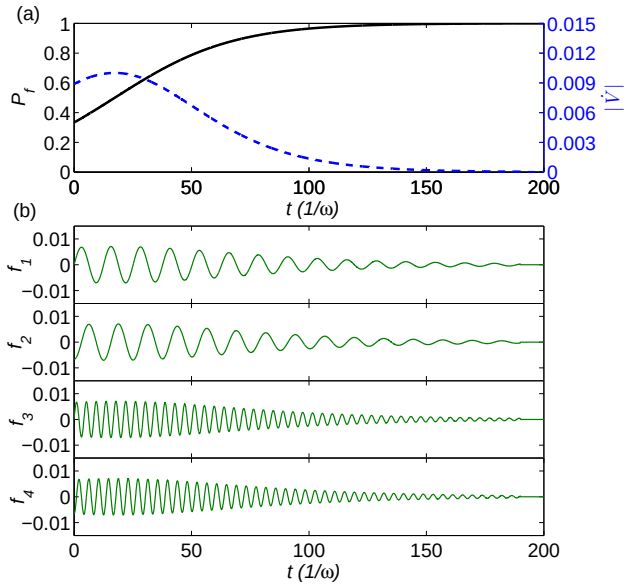

FIG. 1: **(color online)** (a) P_f **(solid line)** and $|\dot{V}|$ **(dashed line)** as a function of time with the conventional control design $f_n(t) = -KT_n$. (b) Control fields **(in units of** ω**)** for W_{max}=0.0001, and $S_{max} = 0.007$. These fields are switched off when $P_f \geq 0.999$ at $t = 191$.

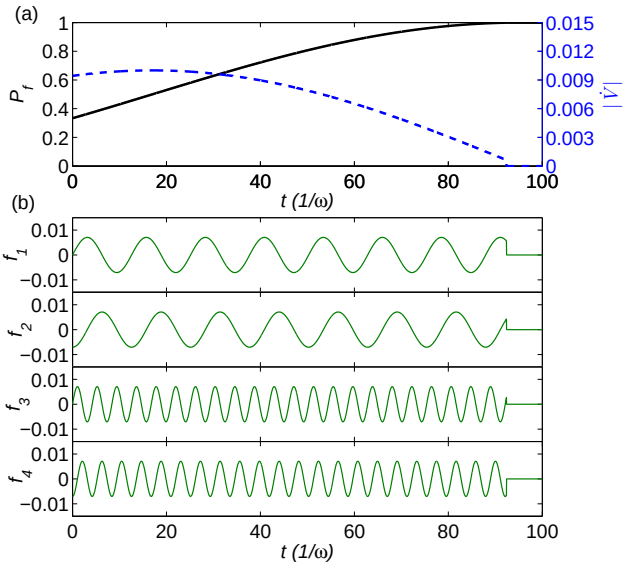

FIG. 2: **(color online)** (a) P_f **(solid line)** and $|\dot{V}|$ **(dashed line)** as a function of time with the control design Eq.(12) under constraint A. (b) Control fields **(in units of** ω**)** with $W_{max} = 0.0001$. These fields are switched off at $t = 90$ when $P_f \geq 0.999$.

According to the Lyapuonv control theory, the system Eq.(17) will be driven to an eigenstate of P with the minimum eigenvalue 0, i.e., $\rho \to \rho_f = |3\rangle\langle 3|$. Additionally, in the pure state case, this Lyapunov function can be explained as the Hilbert Schmidt distance between $|\phi\rangle$ and $|\phi_f\rangle$. Recall that $P = \mathrm{I} - |\phi_f\rangle\langle\phi_f|$, and $V = \mathrm{Tr}(P\rho) = \mathrm{Tr}((\mathrm{I} - |\phi_f\rangle\langle\phi_f|)|\phi\rangle\langle\phi|) = 1 - |\langle\phi|\phi_f\rangle|^2$, our control design in this example acts to make the distance between $|\phi\rangle$ and $|\phi_f\rangle$ decrease as fast as possible with a given restriction on the control fields.

In order to achieve the best performance, we choose the control Hamiltonians H_n to be the generators of the $SU(3)$ group $\lambda_n (n = 1, ..., 8)$, namely, $H_c(t)$ is constrained from

$$\begin{aligned}
\lambda_1 &= \begin{pmatrix} 0 & 1 & 0 \\ 1 & 0 & 0 \\ 0 & 0 & 0 \end{pmatrix}, \quad \lambda_2 = \begin{pmatrix} 0 & -i & 0 \\ i & 0 & 0 \\ 0 & 0 & 0 \end{pmatrix}, \\
\lambda_3 &= \begin{pmatrix} 1 & 0 & 0 \\ 0 & -1 & 0 \\ 0 & 0 & 0 \end{pmatrix}, \quad \lambda_4 = \begin{pmatrix} 0 & 0 & 1 \\ 0 & 0 & 0 \\ 1 & 0 & 0 \end{pmatrix}, \\
\lambda_5 &= \begin{pmatrix} 0 & 0 & -i \\ 0 & 0 & 0 \\ i & 0 & 0 \end{pmatrix}, \quad \lambda_6 = \begin{pmatrix} 0 & 0 & 0 \\ 0 & 0 & 1 \\ 0 & 1 & 0 \end{pmatrix}, \\
\lambda_7 &= \begin{pmatrix} 0 & 0 & 0 \\ 0 & 0 & -i \\ 0 & i & 0 \end{pmatrix}, \lambda_8 = \frac{1}{\sqrt{3}} \begin{pmatrix} 1 & 0 & 0 \\ 0 & 1 & 0 \\ 0 & 0 & -2 \end{pmatrix}.
\end{aligned} \tag{20}$$

Notice that since only $\lambda_1, \lambda_2, \lambda_4$ and λ_5 satisfy $[P, \lambda_n] \neq 0$, only these generators are effective for our model which can be understood by examining Eq.(4). Therefore, the control Hamiltonians are chosen as,

$$\begin{aligned}
H_1 = \lambda_1 = \begin{pmatrix} 0 & 1 & 0 \\ 1 & 0 & 0 \\ 0 & 0 & 0 \end{pmatrix}, H_2 = \lambda_2 = \begin{pmatrix} 0 & -i & 0 \\ i & 0 & 0 \\ 0 & 0 & 0 \end{pmatrix}, \\
H_3 = \lambda_4 = \begin{pmatrix} 0 & 0 & 1 \\ 0 & 0 & 0 \\ 1 & 0 & 0 \end{pmatrix}, H_4 = \lambda_5 = \begin{pmatrix} 0 & 0 & -i \\ 0 & 0 & 0 \\ i & 0 & 0 \end{pmatrix},
\end{aligned} \tag{21}$$

which can be rewritten as $H_1 = |3\rangle\langle 2| + |2\rangle\langle 3|$, $H_2 = i(-|3\rangle\langle 2| + |2\rangle\langle 3|)$, $H_3 = |3\rangle\langle 1| + |1\rangle\langle 3|$, and $H_4 = i(-|3\rangle\langle 1| + |1\rangle\langle 3|)$, which couple the energy levels $|1\rangle$ and $|2\rangle$ to the final state $|3\rangle$. We would like to note that the control Hamiltonians in this example are optimal, because any operator for this 3-level system can be written as an expansion of these generators. For high-dimensional system, the problem becomes more complicated.

We first simulate the problem with the conventional control field design $f_n(t) = -K\mathrm{Tr}(-i\rho[P, H_n])$ with $K = 0.01$ and initial state $|\phi_0\rangle = \frac{1}{\sqrt{3}}(|1\rangle + |2\rangle + |3\rangle)$. The control fields are switched off when the probability $P_f = |\langle\phi|\phi_f\rangle|^2$ reaches 0.999 both in this simulation and the following two so as to compare the evolution time. Fig.1(a) shows the evolution of probability P_f (black solid line) and $|\dot{V}|$ (blue dashed line). It is seen that the system is driven to target state $|\phi_f\rangle$ and the evolution time is about $t = 191$ for $P_f = 0.999$. The time-varying control fields $f_n(t)$ are plotted in Fig.1(b). The power $W = \sum_{n=1}^{4} f_n(t)^2$ reaches its maximum $W_{max} = 0.0001$ at $t = 17$ and the maximal strength of a single control field is $|f_1| = 0.007$ at $t = 16$.

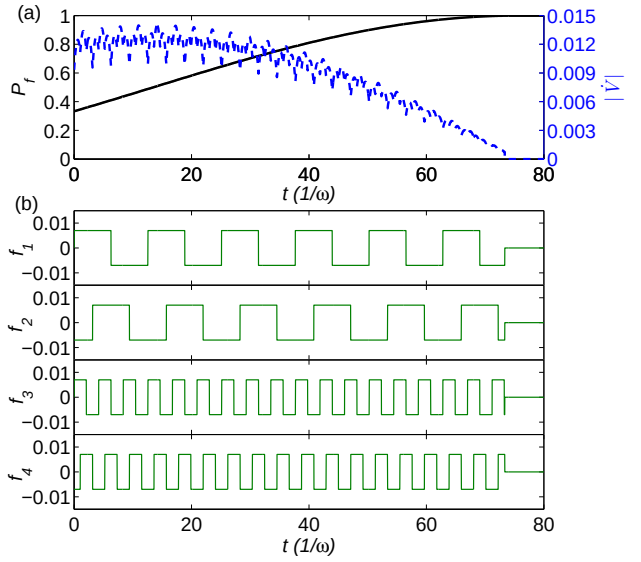

FIG. 3: **(color online)** (a) P_f **(solid line)** and $|\dot{V}|$ **(dashed line)** as a function of time with "bang-bang" control Eq.(15) under constraint B. (b) Control fields **(in units of** ω **)** with $S = 0.007$. These fields are switched off at $t = 74$ when $P_f \geq 0.999$.

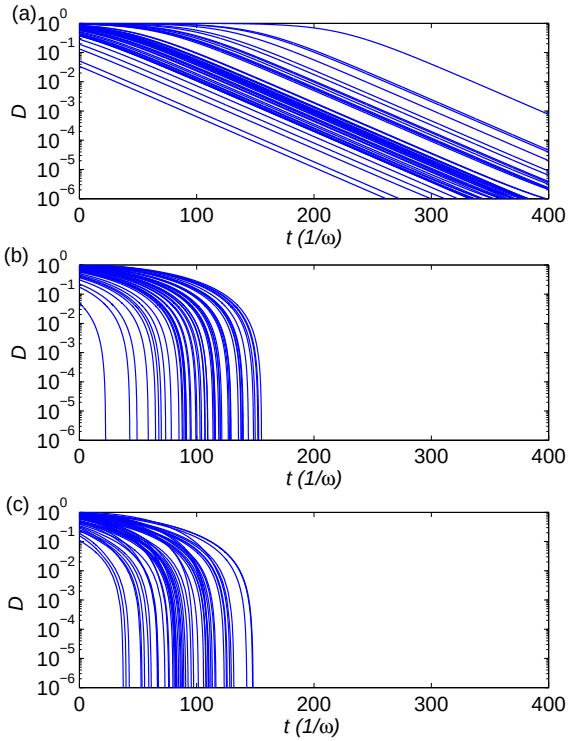

FIG. 4: (color online) Evolution of $D = 1 - |\langle\phi|\phi_f\rangle|^2$ for the three control designs with logarithmic scale. (a),(b) and (c) correspond to the conventional control field design, the design under constraint A, and that under constraint B, respectively. Each picture is a result averaged over 50 random initial states. The convergence speed of (b) and (c) is faster than that of (a) as these figures show.

Next, we employ the control design Eq.(12) under the constraint on the power of control fields. In order to be comparable with the last example, the maximal power W_{max} and initial state are chosen to be the same as the above one. Results in Fig.2(a) show that the evolution time for $P_f = 0.999$ is $t = 92$ which is evidently shorter than that shown in Fig. 1. Control fields are plotted in Fig.2(b) which have a sinusoidal shape. In this example, for all the time before control fields are switched off, the power of control fields remains constant and the shapes of fields are optimized so that the Lyapunov function decreases fastest under constraint A. We can see this from evolution of $|\dot{V}|$ in Fig.2(a) (blue dotted line).

Now we study the control design Eq.(15) under constraint B. For comparison, we let the maximal strength S and the initial state be the same as that in the first simulation. The simulation results are illustrated in Fig.3. The evolution time for $P_f = 0.999$ is $t = 73$ which is about 38 percent of the first example. In this example, the control fields shown in Fig.3(b) are step-like. Such a control method makes Lyapunov function decrease fastest under the restriction of strength and has the advantage of being easy to be implemented in experiment. The evolution of $|\dot{V}|$ is not smooth (shown in Fig.3(a) by blue dashed line), which is due to the discrete control fields.

Furthermore, we plot in Fig.4 the evolution of $D = 1 - |\langle\phi|\phi_f\rangle|^2$ for the three designs of control field with 50 randomly chosen initial states ($|\phi_r\rangle = R[r_1 e^{i2\pi r_4}, r_2 e^{i2\pi r_5}, r_3 e^{i2\pi r_6}]^T$, where $r_i (i = 1, ..., 6)$ are random numbers uniformly created between 0 and 1, $R = \frac{1}{\sqrt{r_1^2+r_2^2+r_3^2}}$ is a normalization factor) respectively. The simulations show that the convergence rate for the usual control design is exponential where the evolution time grows linearly with the distance between the actual and target states D, whereas the convergence rate of our two methods is larger than the conventional one, especially when the control fidelity is required to be high. The reason is our methods keep $|\dot{V}|$ at its maximum for all the evolution even if T_n is very small.

We found that some of the control fields may oscillate with very high frequency at the end of the control in Eq.(15) with constraint B. The oscillation depends on the initial state and the distance between the actual and target states. The reason of this oscillation is as follows. When the state is close to the target state, some T_n become very small leading to ineffectiveness of the corresponding control field $f_n(t)$. While in conventional Lyapunov control, the control field $f_n(t)$ decreases to zero with $T_n \to 0$. In our method, however, $f_n(t)$ is designed to take the value S or $-S$, which makes the state oscillate almost every step of simulation. This problem can be solved by averaging the control fields over a proper time period and then use the reshaped fields instead of

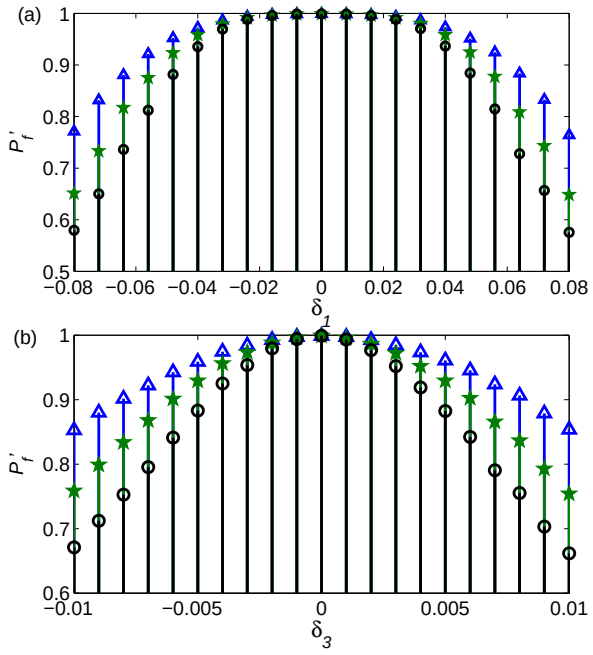

FIG. 5: **(color online)** The average fidelity verses uncertainties in the free Hamiltonian, (a) for λ_1 and (b) for λ_3. The blue triangle, green star and black circle represent the fidelity obtained by bang-bang control design, design with power constraint and the conventional one, respectively.

the oscillating one. In fact, this average can be used in the situation when the control fields are not a (fast) oscillating function of time, it yields the same control fields and maintains the results.

IV. ROBUSTNESS OF THE DESIGNS

One may wonder if these optimal designs improve the robustness of the Lyapunov-based control. In the following, we shall examine this problem following the representations in [26] by calculating an average fidelity of the system with Hamiltonian uncertainties, decoherence and field fluctuation in the controls Eq.(17). Here the average fidelity is defined by $P_f^{'} = \frac{1}{N}(\sum_{j=1}^{N} |\langle\phi_j|\phi_f\rangle|^2)$, $|\phi_j\rangle$ denotes the actual state evolving from a random initial state under the control with uncertainties, decoherence or fluctuations. In other words, the average is taken over N actual states, each evolves from a randomly chosen initial state, driving by the controls with uncertainties, decoherence or fluctuations. Our focus is on whether the optimal designs is robust against these uncertainties compared with the conventional one.

We begin with analyzing robustness against the uncertainty in the free Hamiltonian H_0. The uncertainties can be taken into account by adding a perturbation δH_0 to the free Hamiltonian, i.e.,

$$H_0 \to H_0 + \delta H_0.$$

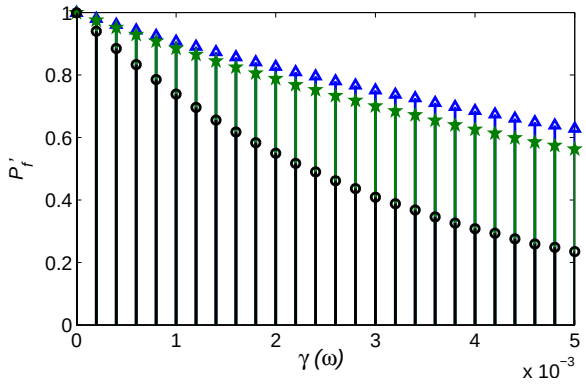

FIG. 6: **(color online)** The average fidelity as a function of the decoherence rates, here we choose $\gamma_2 = \gamma_3 = \gamma$. The blue triangle, green star and black circle represent bang-bang control design, design with power constraint and the conventional one, respectively.

Here $\delta H_0 = \sum_{n=1}^{8} \delta_n \lambda_n$ with δ_n a real number and λ_n the generators in Eq.(20). For simplicity, we examine separately the 8 uncertainties $\delta H_0 = \delta_n \lambda_n$, $n = 1, 2 \cdots 8$. The equation $\frac{d\rho}{dt} = -i[H_0 + \delta H_0 + \sum_{n=1}^{4} f_n(t) H_n, \rho]$ is simulated for the three designs with the same control fields and the same parameters as in section III. Selected results are showed in Fig.5 where the fidelity $P_f^{'}$ is an average over fidelities from 1000 randomly chosen initial states.

The simulations show that, (1) the optimal Lyapunov control is robust against the uncertainty λ_1, and is sensitive to that of λ_3; (2) the bang-bang design is more robust than the design with power constraint, and the conventional design has the worst robustness. In fact, the robustness against the uncertainty $\delta_8\lambda_8$ is similar to Fig.5(a) and robustness against the uncertainties $\delta_n\lambda_n (n = 2, 3, 4, 5, 6, 7)$ is roughly similar to Fig.5(b). Thus here we only show the robustness of the control against the uncertainties λ_1 and λ_3. This conclusion confirms that the system is sensitive to the uncertainties that commute with the free Hamiltonian, while it is robust against the uncertainties that does not.

We next discuss the robustness against decoherence. In this discussion, we assume that states $|2\rangle$ and $|1\rangle$ are long lived, namely only the spontaneous emission $|3\rangle \to |1\rangle$ and $|3\rangle \to |2\rangle$ is assumed. This can be described by $\mathcal{L}(\rho) = \sum_{i=1,2} \gamma_i (\sigma_i^- \rho \sigma_i^+ - \frac{1}{2}\sigma_i^- \rho \sigma_i^+ - \frac{1}{2}\sigma_i^- \rho \sigma_i^+)$ with $\sigma_i^- = |i\rangle\langle 3|$ and $\sigma_i^+ = |3\rangle\langle i|$. With this assumption, the target state is not a steady state, so the fidelity will be affected seriously. However, the optimal controls are better than the conventional one due to the short time needed to drive the quantum system from an initial state to the target state. As we did in Fig.5, we calculate the average fidelity for the three control designs with 1000 random initial state and fixed γ. The results are depicted in Fig.6. In this case, the fidelity of the two optimal designs is obviously higher than the conventional design.

The robustness against field fluctuations (with zero-mean) and errors in the initial state is also explored. The results are similar to that in [26], namely the control field fluctuation with zero mean affects the fidelity slightly, while it depends sharply on the fluctuation with non-zero mean, and the final fidelity is sensitive to the initial state. In these cases, the optimal control has no advantage with respect to the conventional one.

V. APPLICATION TO THE COOLING OF A MECHANICAL OSCILLATOR

The cooling of mechanical resonators [27–31] becomes an active research topic in recent years due to its potential applications in detecting extremely small displacement and observing quantum phenomenon of macroscopic mechanical object. In this section, we apply the Lyapunov control to cooling a nano-mechanical resonator. The results show that it is possible to cool a nano-mechanical system to its ground state by Lyapunov control, the optimized control design leads to a shorter cooling time with respect to the conventional control design.

Consider a nano-mechanical resonator (called target) with frequency ω coupled to the other microwave (optical) oscillator (auxiliary system), the microwave oscillator has a sufficiently higher frequency Ω such that it can be prepared in its ground state at finite temperature. In the language of Lyapunov control, the free Hamiltonian of the composite system is given by

$$H_0 = \hbar\omega a^\dagger a + \hbar\Omega b^\dagger b. \tag{22}$$

We assume the coupling Hamiltonian of the two oscillators has the following form,

$$H_c = g(t)x_A x_B \tag{23}$$

with $x_A = a + a^\dagger$ and $x_B = b + b^\dagger$. This type of Hamiltonian can be realized by coupling the target to a LC oscillator and the coupling rate $g(t)$ can be modulated by the voltage of the LC circuit [27–29].

In the sideband cooling, $g(t)$ is modulated at $\Omega - \omega$ so that the two resonators are effectively coupled and the rotating wave approximation (RWA) applies when the coupling g is weak. Recently, the authors of [27] shown that quantum control can improve the cooling, when the control goes beyond the RWA in the ultra-strong coupling regime $g \sim \omega$ [27]. Here, we show that we can obtain the control design by the Lyapunov functional, and the optimized Lyapunov design can shorten the cooling time.

Denote the state of the two resonators by ρ, we can choose the Lyapunov function as

$$V(\rho) = \mathrm{Tr}(a^\dagger a\rho) = \langle n_a\rangle, \tag{24}$$

namely, we choose the mean phonon number of the target resonator as the Lyapunov function, which is non-negative and becomes zero when the target system is cooled to its ground state. By the same procedure, we get

$$\dot{V}(\rho) = g(t)T_n. \tag{25}$$

Here $T_n = \mathrm{Tr}(-i\rho[a^\dagger a, (a^\dagger + a)(b^\dagger + b)])$. If $g(t)$ is chosen to keep $\dot{V} \leq 0$, the phonon number of target resonator will decrease monotonically. The conventional Lyapunov design for the time-dependent coupling strength is $g(t) = -KT_n$ with K a positive constant, while the optimal Lyapunov design is a *bang-bang* control given by Eq.(15).

Assume that the target resonator is initially in a thermal state with average phonon number $\langle n_a\rangle = 6.38$ and the auxiliary system is prepared in its ground state. Note that the frequency of auxiliary system Ω should be sufficiently large compared with ω, such that thermal fluctuation has small effect on the microwave oscillator. Our numerical simulations show that larger Ω leads to faster oscillation of $g(t)$, but it does not affect the cooling results. Here we set $\Omega/\omega = 20$.

The simulations are performed in the Fock space, we truncate the Fock space of each oscillator up to 20 Fock states and the dissipation of each resonator is ignored. Compare to simulations with 25-Fock state-truncations, improvement is not significant, so the simulations with

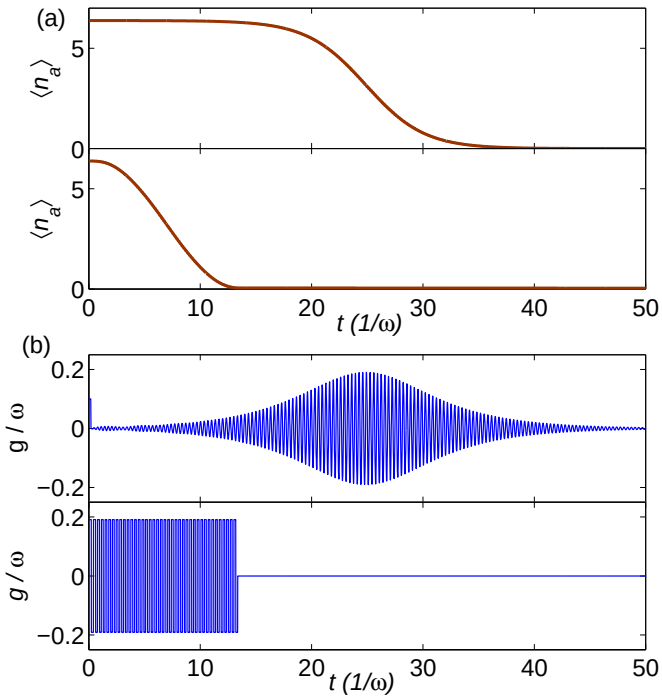

FIG. 7: (color online) (a) Phonon number versus time for the conventional Lyapunov design (upper half) and optimal Lyapunov design (lower half). The evolution time for $\langle n_a\rangle = 0.05$ is $\omega t = 37.5$ (upper) and $\omega t = 13.4$ (lower), respectively. (b) Time-dependent coupling for the conventional design (upper) and the optimal design (lower), where $g(t)$ for the two designs share the same maximal strength $|g_{max}|/\omega = 1.91$. $g(t)$ for the optimal design is shut off after $\omega t = 13.4$.

20-Fock state-truncation are reasonable. We compare the evolution of phonon number $\langle n_a \rangle$ and $g(t)$ for the two designs in Fig.7. The top half of Fig.7(a) represents the evolution of $\langle n_a \rangle$ for conventional design with $K = 0.03$ and maximal control field strength $|g(t)|/\omega = 0.191$. It takes $t = 37.5$ (in unit of $1/\omega$) for the target to reach $\langle n_a \rangle = 0.05$. In contrast, for the optimal design, the evolution time for reaching the same phonon number is $t = 13.4$ as shown in the lower half of Fig.7(a). Obviously the optimal Lyapunov design shorten the cooling time. Fig.7(b) shows the time dependence of $g(t)$ for the conventional (upper half) and optimal (lower half) design. For each case, the control field $g(t)$ starts with a non-zero small number to avoid $T_n = 0$ at the initial time. It is seen that the optimal Lyapunov design leads to a faster decrease of Lyapunov function (i.e. the phonon number). In addition, the major components of the oscillation frequency of $g(t)$ is automatically turned to the frequency difference $\Omega - \omega$ of the two resonators(like that in the sideband cooling scheme).

VI. SUMMARY

We have presented two designs for Lyapunov control under constraints on the total power and individual strength of the control fields. These designs make Lyapunov function decrease fastest determined by the constraints. It has been shown that the implementation of our designs leads to a shorter time towards the target state especially for high fidelity requirement. Moreover, the second control design gives simple *bang-bang* control fields, which may be easy to implement in experiment. Intuitively, our methods use a constant power or strength of control fields to make Lyapunov function decrease as fast as possible. This optimal control is more robust against uncertainties in the Hamiltonian and decoherence in the system with respect to the conventional design. **We also explore the application of our optimal design to cool a nanomechanical system, a significantly shorter time is obtained compared with the conventional Lyapunov design.** Here we focused only on how to design control fields with fixed control Hamiltonian H_n, a general formalism to choose control Hamiltonian H_n to speed up Lyapunov control is still an open issue.

This work is supported by NSF of China under grant Nos 61078011, 10935010 and 11175032, and the Australian Research Council.

[1] D. D'Alessandro, *Introduction to Quantum Control and Dynamics* (Taylor and Francis Group, Boca Raton London New York 2007).
[2] D. Dong, and I. R. Petersen, IET Control Theory Appl. **4**, 12 2651 (2010).
[3] A. Carlini, A. Hosoya, T. Koike, and Y. Okudaira, Phys. Rev. Lett. **96**, 060503 (2006).
[4] N. Khaneja, R. Brockett, and S. J. Glaser, Phys. Rev. A **63**, 032308 (2001).
[5] D. D'Alessandro, and M. Dahleh, IEEE Transactions on Automatic Control, **46**, 6 (2001).
[6] J. P. Palao, and R. Kosloff, Phys. Rev. Lett. **89**, 18 (2002).
[7] S. G. Schirmer, A. D. Greentree, V. Ramakrishna, and H. Rabitz, J. Phys. A: Math. Gen. **35**, 8315 (2002).
[8] Weiwei Zhou, S. G. Schirmer, Ming Zhang, and Hong-Yi Dai, J. Phys. A: Math. Theor. **44**, 105303 (2011).
[9] C. K. Law, and J. H. Eberly, Phys. Rev. Lett. **76**, 7 (1996).
[10] S. L. Liao, T. S. Ho, S. I. Chu, and H. Rabitz, Phys. Rev. A **84**, 031401 (2011).
[11] A. Pechen, Phys. Rev. A **84**, 042106 (2011).
[12] D. Dong, and I. R. Petersen, New J. Phys. **11**, 105033 (2009).
[13] F. Verstraete, M. M. Wolf, and J. I. Cirac, Nat. Phys. **5**, 633 (2009).
[14] S. Grivopoulos, and B. Bamieh, Proceedings of the 42nd IEEE Conference on Decision and Control (2003).
[15] P. Vettori, Proceedings of the MTNS Conference (2002).
[16] M. Mirrahimi, P. Rouchou, and G. Turinici, Automatica **41**, 1987 (2005).
[17] X. Wang, and S. G. Schirmer, IEEE Transactions on Automatic Control **55**, 2259 (2010).
[18] X. Wang, and S. G. Schirmer, ENOC 2008, Saint Petersburg, Russia, June, 30-July, 4 (2008).
[19] S. Kuang, and S. Cong, Automatica **44**, 98 (2008).
[20] S. Cong, and S. Kuang, Acta Automatica Sinica, **33** 1 (2007).
[21] X. Wang, and S. G. Schirmer, Phys. Rev. A **80**, 042305 (2009).
[22] W. Wang, L. C. Wang, and X. X. Yi, Phys. Rev. A **82**, 034308 (2007).
[23] X. X. Yi, S. L. Wu, Chunfeng. Wu, X. L. Feng, and C. H. Oh, J. Phys. B: At. Mol. Opt. Phys. **44**, 195503 (2011).
[24] J. M. Coron, A. Grigoriu, C. Lefter, and B. Turinici, New J. Phys. **11**, 105034 (2009).
[25] K. Beauchard, J. M. Coron, M. Mirrahimi, and P. Rouchon, Systems & Control Letters. **55**, 5 388 (2007).
[26] X. X. Yi, B. Cui, Chunfeng. Wu, and C. H. Oh, J. Phys. B: At. Mol. Opt. Phys. **44**, 165503 (2011).
[27] X. Wang, S. Vinjanampathy, F. W. Strauch, and K. Jacobs, Phys. Rev. Lett. **107**, 177204 (2011).
[28] K. Jacobs, H. I. Nurdin, F. W. Strauch, and M. James, arXiv: 1003.2653.
[29] L. Tian, Phys. Rev. B **79**, 103407 (2009).
[30] I. Wilson-Rae, P. Zoller, and A. Imamoḡlu, Phys. Rev. Lett. **92**, 7 (2004).
[31] A. Schliesser, R. Rivière, G. Anetsberger, O. Arcizet, and T. J. Kippenberg, Nature Physics, **4**, 415 (2008).